CHEMICAL ENGINEERING TRANSACTIONS
VOL. 65, 2018
A publication of AIDIC
The Italian Association of Chemical Engineering
Online at www.aidic.it/cet
Guest Editors: Eliseo Ranzi, Mario Costa

ISBN 978-88-95608- 62-4; **ISSN** 2283-9216

Experimental and Kinetic Modeling Study of Pyrolysis and Combustion of Anisole

Matteo Pelucchi[a*], Tiziano Faravelli[a], Alessio Frassoldati[a], Eliseo Ranzi[a], Gorugantu SriBala[b], Guy B. Marin[b], Kevin M. Van Geem[b]

[a] Department of Chemistry, Materials, and Chemical Engineering, Politecnico di Milano, Italy
[b] Department of Materials, Textiles and Chemical Engineering, Gent University, Belgium
matteo.pelucchi@polimi.it

Fast biomass pyrolysis is an effective process with high yields of bio-oil, and is a promising technology to partially replace non-renewable fossil fuels. Bio-oils are complex mixtures with a large amount of oxygenated organic species, such as esters, ethers, aldehydes, ketones, carboxylic acids, alcohols, and substituted aromatic components. Anisole is a simple surrogate of primary tar from lignin pyrolysis and it is very useful to investigate gas-phase reactions of methoxy-phenol species, expected precursors of poly-cyclic aromatic hydrocarbons (PAH) and soot during biomass pyrolysis and bio-oil combustion. This work first presents new pyrolysis data obtained in the Ghent flow reactor, and then it discusses a detailed kinetic mechanism of anisole pyrolysis and oxidation. This scheme is further validated and compared, not only with these pyrolysis data, but also with recently published data of anisole oxidation in jet stirred reactors. Ignition delay time and laminar flame speed computations complement these detailed comparisons. This kinetic mechanism is a first step and places the basis towards a successive model extension to catechol, guaiacol, and vanillin, as representative phenolic components of bio-oil from biomass.

1. Introduction

Fast pyrolysis is an effective biomass conversion process with 70–80% liquid yield, and a high ratio of fuel to feed. It is one of the promising technologies to compete with and partially replace non-renewable fossil fuel resources. Bio-oils are complex mixtures with a great amount of large size oxygenated molecules, which nearly involve all oxygenated organic species, such as esters, ethers, aldehydes, ketones, carboxylic acids, alcohols, and phenols. Together with levoglucosan, furfural, and aldehydes, bio-oil typically contains significant amounts of phenols with methoxy groups (~30% wt, as in Bertero et al. (2012)), typical decomposition products of lignin components. Substituted phenolic species are also obtained in similar amounts from the conversion of Arundo Donax L. to levulinic acid (Licursi et al., 2015). Mainly for this reason and since several years, anisole was selected as a reference species (Suryan et al., 1988; Pecullan et al., 1998; Barker-Hemings et al., 2012; Nowakoska et al., 2014). In fact, anisole is a simple surrogate of primary tar from lignin pyrolysis and it is very useful to investigate the gas-phase reactions of methoxy-phenol species forming PAH and soot during biomass pyrolysis and combustion. Figure 1 shows examples of aromatic and phenolic species useful to characterize the pyrolysis and combustion behavior of tar species released from biomass pyrolysis. This paper first presents new experimental data on anisole pyrolysis obtained in the flow reactor at Ghent University, then it analyzes and discusses the detailed kinetic mechanism of pyrolysis and oxidation of anisole, also based on several comparisons with experimental data allowing to derive rate rules for the major reaction classes.

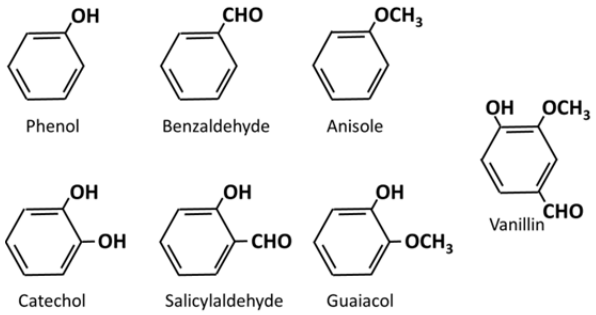

Figure 1: Reference and typical phenolic and aromatic substituted components useful to characterize bio-oil.

2. Pyrolysis of anisole in a flow reactor

New experimental data of anisole pyrolysis are obtained on a bench-scale pyrolysis reactor setup, schematically represented in Figure 2. The pyrolysis reactor is made of Incoloy 800HT, 1.475 m long, with an internal diameter of 6 mm. Anisole and nitrogen are initially pre-heated up to 250 °C and then fed to the tubular flow reactor, monitoring mass flow with Coriflow mass flow controllers. The reactor furnace is divided into eight separate sections, which are electrically heated to set any type of temperature profile. Eight thermocouples located along the reactor coil measure the temperature profile of the reacting gases.

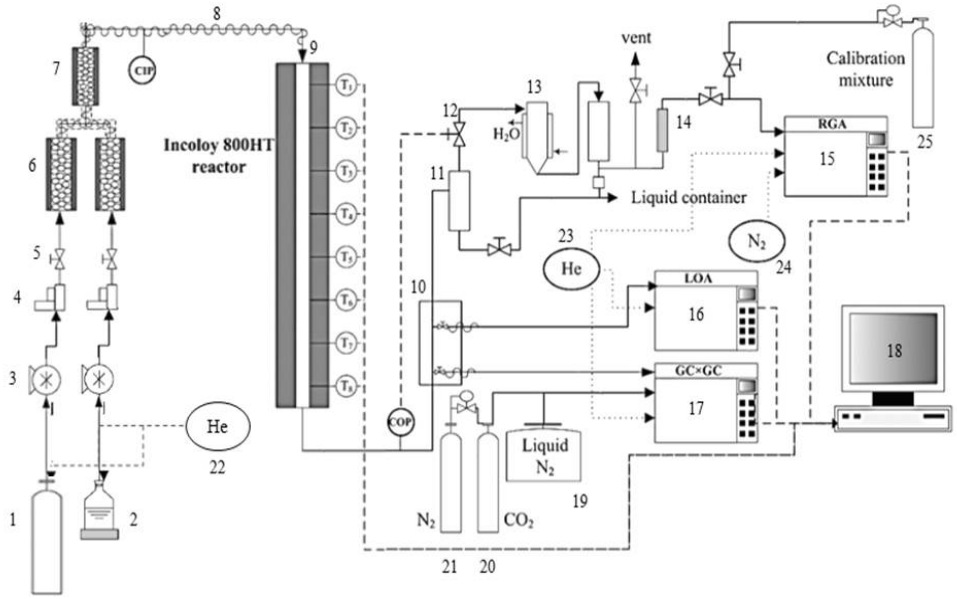

Figure 2: Schematic diagram of the bench-scale setup for anisole pyrolysis (1-N_2; 2-Anisole; 3-pump; 4-massflow controller; 5-valve; 6-evaporator; 7-mixer; 8-heater; 9-reactor; 10-samplebox; 11-cyclone separator; 12-pressure regulator; 13-condenser; 14-dehydrator; 15-RGA GC for C_4^-; 16-LOA GC for light oxygenates, 17-GC × GC for C_5^+; 18-data acquisition system, 19-liquid N_2 supply to cool GC × GC, 20- CO_2 and 21-N_2 supply for modulation of GC×GC, 22-He supply for pressurizing feed, 23-He carrier gas supply to 3 GCs, 24-N_2 carrier gas supply to RGA, 25-calibration gas mixtures to RGA).

The analysis section consists of a refinery gas analyzer (RGA), light oxygenate analyzer (LOA) and a GC x GC-FID/TOF-MS which enable both qualification and quantification of the entire product stream. The reactor effluent is sampled on-line at a temperature of 260°C. Quantification of C_{4-} effluent gases was performed using RGA, whereas the C_{5+} fraction was analyzed using GC x GC-FID/TOF-MS. The RGA was calibrated using a standard calibration gas mixture and C_{5+} fraction is quantified using effective carbon number method. Details of these analytical instruments and quantification methods have been discussed elsewhere (Van Geem et. al., 2010; Pyl et al., 2011; Djokic et al., 2013). Figure 3 illustrates the GC x GC analysis of anisole pyrolysis, showing product composition and emphasizing the PAH formation. Polycyclic aromatics like benzofuran, dibenzofuran and biphenyl with oxygenated side chains were also identified (SriBala et al., 2016).

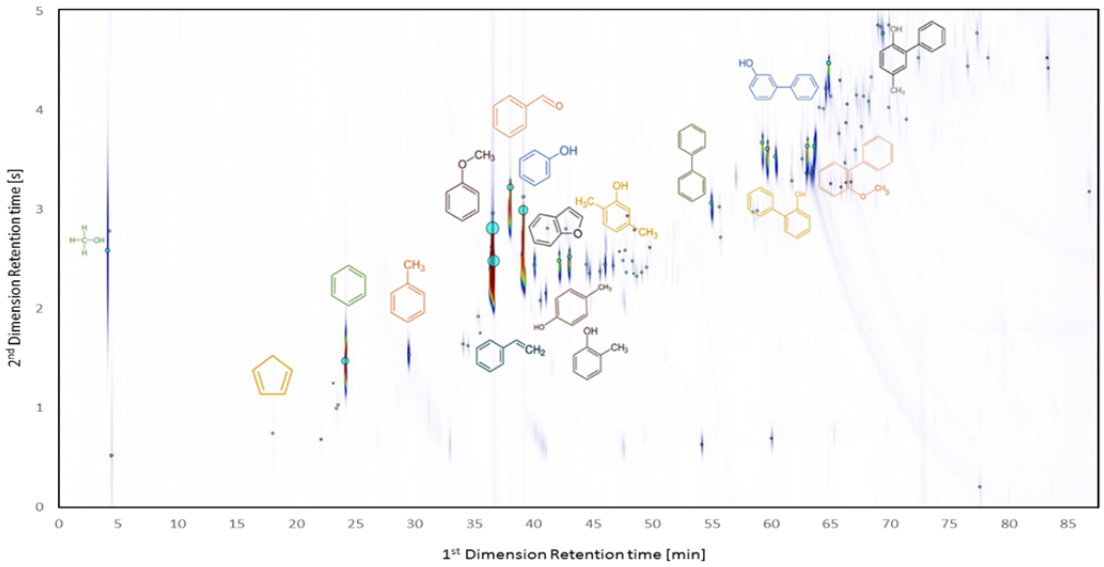

Figure 3. GC x GC- FID chromatogram of anisole pyrolysis showing product composition at a reactor temperature of 675 ˚C.

3. Kinetic mechanism of pyrolysis and oxidation of anisole

Table 1 shows relevant reactions of anisole pyrolysis and oxidation (Baker-Hemings et al., 2011), which are here revised and coupled with the more general CRECK kinetic scheme (POLI_1710), recently modified to include the C_0-C_2 core developed at National University of Ireland, Galway (Keromnes et al. Combust Flame 2013, Burke et al. Combust Flame 2014). The overall kinetic scheme is available upon request to the authors.

Table 1: Relevant reactions in pyrolysis and combustion of anisole (after Barker Hemings et al. (2011)). Units are l/mol/cal/s.

#	Reaction	A	Ea [cal/mol]
1	C6H5OCH3 → C6H5O+CH3	5.00E+15	64700
2	CH3+C6H5O → CH3C6H4OH	1.50E+09	0
3	H+C6H5OCH3 → C6H6+CH3O	1.20E+10	5500
4	H+C6H5OCH3 → H+CH3C6H4OH	1.00E+09	5000
5	OH+C6H5OCH3 → C6H5OH+CH3O	1.00E+10	5000
6	H+C6H5OCH3 → H2+C6H5OCH2	7.10E+10	10500
7	CH3+C6H5OCH3 →	1.20E+09	11500
8	CH4+C6H5OCH2	1.20E+10	3500
9	OH+C6H5OCH3 →	1.60E+09	19000
10	H2O+C6H5OCH2	5.00E+10	49000
11	HO2+C6H5OCH3 →	6.00E+11	0
12	H2O2+C6H5OCH2	5.00E+11	43920
13	O2+C6H5OCH3 →	1.50E+11	0
	HO2+C6H5OCH2		
	H+C6H5O → C6H5OH		
	C6H5O → cy-C5H5+CO		
	H+C6H5O → cy-C5H6+CO		

Anisole decomposition mainly occurs through the thermal homolysis of the relatively weak C-O bond of methoxy group, according to the reaction (R1): $C_6H_5OCH_3 \rightarrow C_6H_5O + CH_3$. Suryan et al. (1989) already observed that the fission of the C-O bond accounts for the extensive conversion of anisole and the formation of the resonantly stabilized phenoxy radical C_6H_5O, with a resonance energy of ~17.5 kcal/mol (Pecullan et al., 1997). Figure 4 shows comparisons between experiments and model predictions. Interactions between phenol and C_2 species form benzofuran, whereas dibenzofuran is mainly formed from self-recombination reactions of phenoxy radicals.

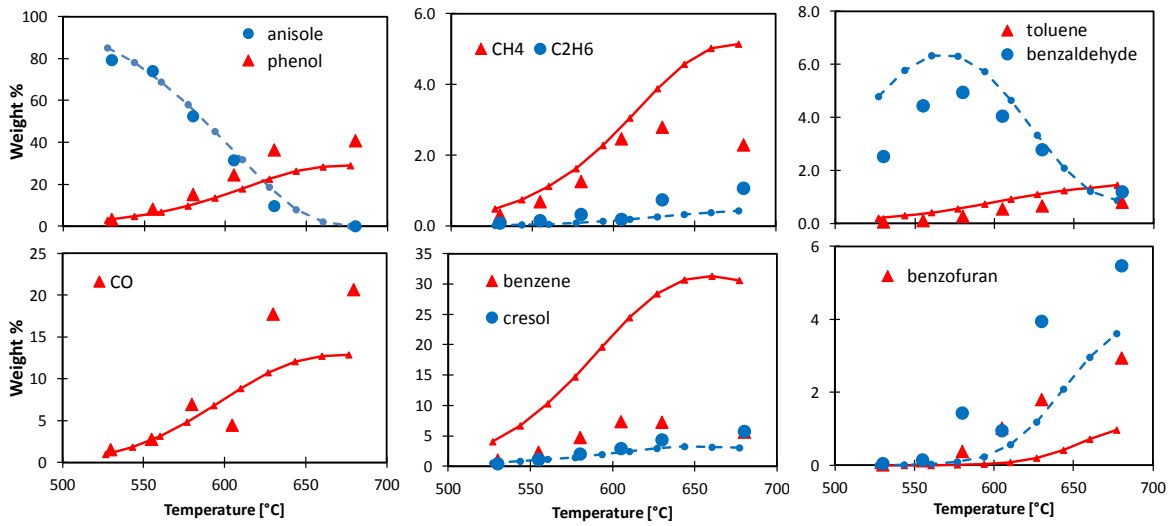

Figure 4. Anisole pyrolysis in Gent flow reactor. Comparisons between experimental data (symbols) and model predictions (lines).

4. Comparisons with experimental data

Model simulations presented hereafter have been performed with the OpenSMOKE++ code of Cuoci et al. (2015). Figure 5 shows a comparison of model predictions both with the pyrolysis and oxidation data of Nowakowska et al. (2014). These JSR Nancy experiments were performed in the temperature range 673–1173 K at constant pressure (106.7 kPa), and residence time of 2 s for both pyrolysis and oxidation conditions. More recent data of Wagnon et al. (2017) have also been used to further validate the model. Model predictions are reasonably within the experimental deviations.

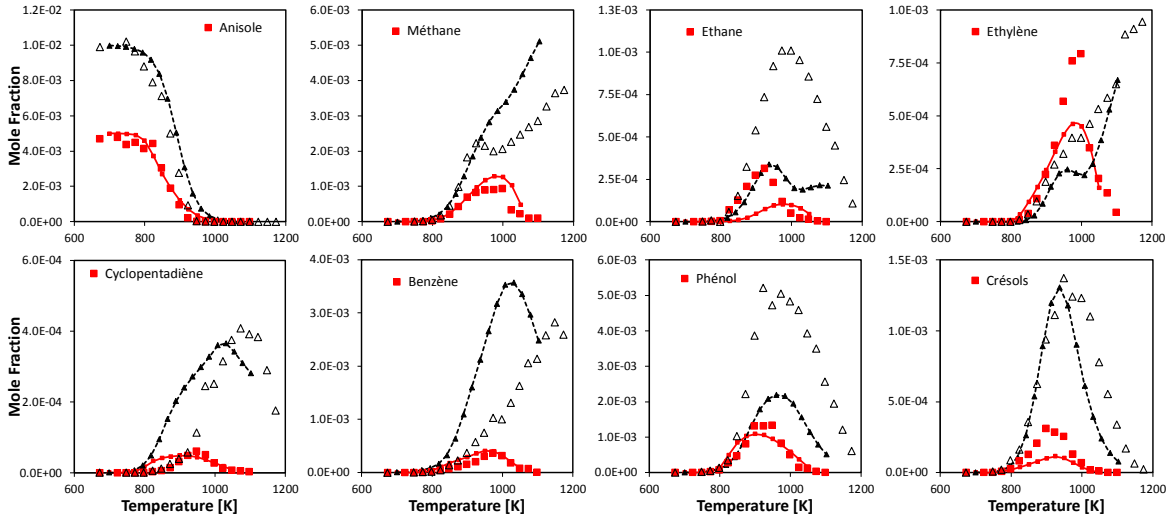

Figure 5. Anisole pyrolysis (triangles) and oxidation (squares) in Nancy JSR (Nowakowska et al. 2014). Comparisons between experimental data (symbols) and model predictions (lines).

Shu et al. (2017) recently measured ignition delay times of anisole/air mixtures at various equivalence ratios (φ) and reflected shock pressure (p=10, 20 and 40 bar) in the temperature range 900-1600 K. Figure 6 shows the satisfactorily agreement between measurements and model predictions at φ=0.5. Deviations are observed for long ignition time (> 1 ms), due to non-idealities of the experimental apparatus such as earlier pressure rise prior to shock arrival, because of pre-ignitions (Davidson and Hanson, 2004). More than the effect of unlikely low temperature reactions, the inclusion of facility effects in terms of pressure variation over time would improve such comparisons.

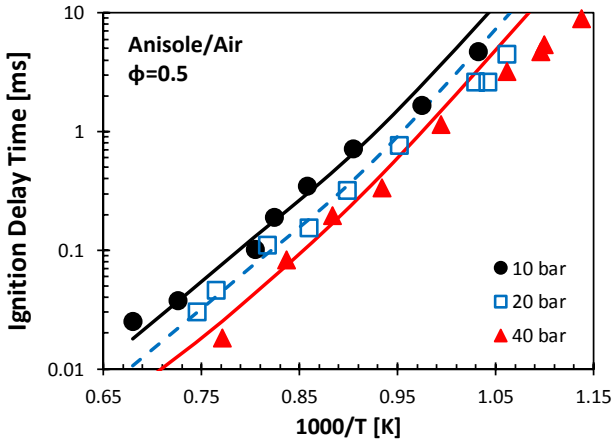

Figure 6. Ignition Delay Time of anisole/air mixtures at φ=0.5, at p=10, 20 and 40 bar (Shu et al., 2017). Comparisons of experimental data (symbols) and constant volume simulations (lines).

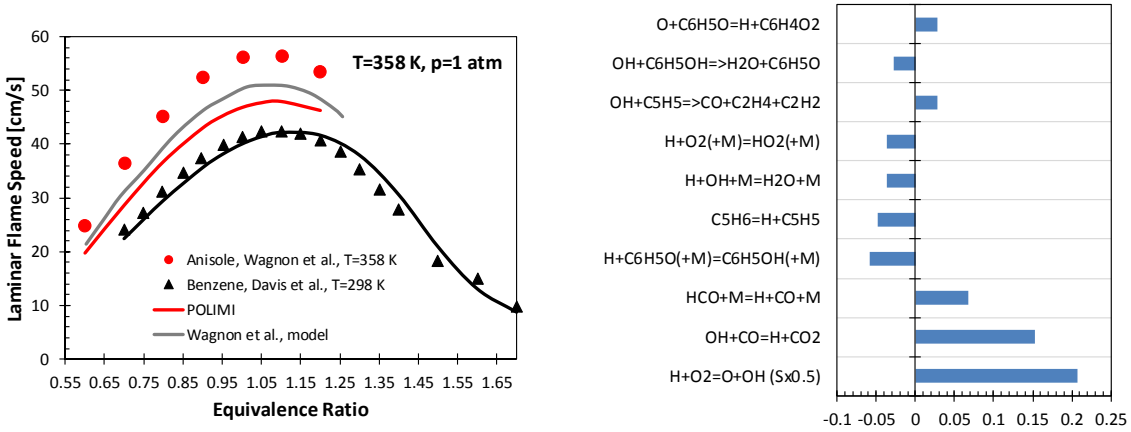

Figure 7. Laminar flame speed. Comparisons of experimental data (symbols) and model predictions (lines). Sensitivity coefficients of laminar flame speed at φ=1.1

Figure 7 compares predicted and experimental premixed laminar burning speed, as measured on a heat flux stabilized burner at an unburnt temperature of 358 K and 1 bar (Wagnon et al. 2017). Model underestimations are even higher than the ones already observed by Wagnon. To highlight kinetic reasons behind such deviations, sensitivity coefficients for the case at φ=1.1 are also reported in the figure. Beside key reactions belonging to the C_0-C_2 core mechanism, none of fuel specific reactions appears in the top ten most sensitive reactions. However, the phenol and cyclopentadiene sub-mechanisms show some importance, and they require a specific and careful attention. The recombination of H radicals with phenoxy and cyclopentadienyl radicals significantly reduce anisole laminar flame speed, but they also control benzene flame reactivity (Ranzi et al., 2012).

5. Conclusions

This study presents an update and extension of anisole pyrolysis and oxidation kinetic mechanism together with new experimental measurements in a flow reactor. The kinetic mechanisms of anisole are mainly derived from the gas–phase reactions of phenol and aromatic components. Due to the hierarchical structure of detailed kinetic mechanisms, these subsets will constitute the basis for the successive extension of the kinetic scheme to describe the pyrolysis and oxidation of more representative and substituted aromatic compounds found in bio-oils such as guaiacol (2-metoxy-phenol), catechol (2-hydroxy-phenol), and vanillin (4-hydroxy-3-methoxy-benzaldehyde: $C_8H_8O_3$).

Acknowledgments

The authors gratefully acknowledge the partial financial support for this research provided by the European Union under the Horizon 2020 research and innovation programme (Residue2Heat project, G.A. No 654650). This work was partly supported by the 'Long Term Structural Methusalem Funding by the Flemish Government'. The SBO proposal “Bioleum” supported by the Institute for promotion of Innovation through Science and Technology in Flanders (IWT) is also acknowledged by GS, GBM and KVG.

References

Barker Hemings, E., Bozzano, G., Dente, M. and Ranzi, E., 2011. Detailed kinetics of the pyrolysis and oxidation of anisole. Chem. Eng. Trans, 24, pp.61-66.

Bertero, M., de la Puente, G., & Sedran, U., 2012. Fuels from bio-oils: Bio-oil production from different residual sources, characterization and thermal conditioning. Fuel, 95, pp.263-271.

Cuoci, A., Frassoldati, A., Faravelli, T. and Ranzi, E., 2015. OpenSMOKE++: An object-oriented framework for the numerical modeling of reactive systems with detailed kinetic mechanisms. Computer Physics Communications, 192, pp.237-264.

Davidson, D. F., & Hanson, R. K. (2004). Interpreting shock tube ignition data. International Journal of Chemical Kinetics, 36(9), 510-523.

Djokic, M., et al., *The thermal decomposition of 2, 5-dimethylfuran.* Proceedings of the Combustion Institute, 2013. 34(1): p. 251-258.

Licursi, D., Antonetti, C., Bernardini, J., Cinelli, P., Coltelli, M. B., Lazzeri, A., Martinelli, M. & Galletti, A. M. R. 2015. Characterization of the Arundo donax L. solid residue from hydrothermal conversion: Comparison with technical lignins and application perspectives. Industrial Crops and Products, 76, pp. 1008-1024.

Nowakowska, M., Herbinet, O., Dufour, A. and Glaude, P.A., 2014. Detailed kinetic study of anisole pyrolysis and oxidation to understand tar formation during biomass combustion and gasification. Combustion and Flame, 161(6), pp.1474-1488.

Pecullan, M., Brezinsky, K. and Glassman, I., 1997. Pyrolysis and oxidation of anisole near 1000 K. The Journal of Physical Chemistry A, 101(18), pp.3305-3316.Suryan et al., 1988;

Pyl, S.P., et al., *Rapeseed oil methyl ester pyrolysis: On-line product analysis using comprehensive two-dimensional gas chromatography.* Journal of Chromatography A, 2011. 1218(21): p. 3217-3223.

Shu, B., Herzler, J., Peukert, S., Fikri, M., & Schulz, C. (2017). A Shock Tube and Modeling Study about Anisole Pyrolysis Using Time-Resolved CO Absorption Measurements. International Journal of Chemical Kinetics, 49(9), 656-667.

Ranzi, E., Frassoldati, A., Grana, R., Cuoci, A., Faravelli, T., Kelley, A. P., & Law, C. K. (2012). Hierarchical and comparative kinetic modeling of laminar flame speeds of hydrocarbon and oxygenated fuels. Progress in Energy and Combustion Science, 38(4), 468-501.

SriBala, G., De Bruycker, R., Carstensen, H.H., Van Geem, K.M. and Marin, G.B., 2016. Single event microkinetic modeling of lignin fast pyrolysis: a study on anisole as model compound. In Thermochemical Lignocellulose Conversion Technologies (CASCATBEL) (pp. 49-49).

Suryan, M.M., Kafafi, S.A. and Stein, S.E., 1989. Dissociation of substituted anisoles: substituent effects on bond strengths. Journal of the American Chemical Society, 111(13), pp.4594-4600.

Van Geem, K.M., et al., *On-line analysis of complex hydrocarbon mixtures using comprehensive two-dimensional gas chromatography.* Journal of Chromatography A, 2010. 1217(43): p. 6623-6633.

Wagnon, S.W., Thion, S., Nilsson, E.K., Mehl, M., Serinyel, Z., Zhang, K., Dagaut, P., Konnov, A.A., Dayma, G. and Pitz, W.J., 2017. The Development and Validation of a Chemical Kinetic Model for Anisole, a Compound to Represent Biomass Pyrolysis Fuels (No. LLNL-CONF-725097). Lawrence Livermore National Laboratory (LLNL), Livermore, CA.